Theoretical investigation of the electronic structure of NiO by ab initio molecular-orbital

calculations

Theoretical investigation of the electronic structure of NiO by *ab initio* molecular-orbital calculations

Hidekazu Takahashi, Fumio Munakata and Mitsugu Yamanaka

Scientific Research Laboratory, Nissan Motor Co. Ltd, 1 Natsushima-cho, Yokosuka 237, Japan

Abstract. The electronic structure of NiO near the Fermi level was investigated by *ab initio* molecular-orbital calculations using the unrestricted Hartree–Fock (UHF) method with basis sets appropriate for nickel and oxygen atoms in order to explain why NiO behaves as an insulator. In the present analysis, we used a cluster composed of finite unit cells of NiO containing the $[Ni-O_6]^{10-}$ cluster. We obtained the result that NiO was an insulator, with a band structure where the upper Ni 3d band was above the Fermi level, and the upper O 2p, the lower O 2p and the lower Ni 3d bands were below the Fermi level. These results were in good agreement with the experimental results obtained by photoelectron spectroscopy (PES) and bremsstrahlung isochromat spectroscopy (BIS), and with the electronic structures derived from the charge-transfer model proposed by Sawatzky and Allen. The main peak observed in PES corresponds to the d^8L state, i.e. O 2p band, and the satellite peaks correspond mainly to the mixed state produced by the correlation between the 2p state of O atoms and the d^8 state of Ni atoms.

1. Introduction

Since de Boer and Verwey [1] pointed out that it was difficult to explain why many compounds such as NiO behaved as insulators using the Wilson and Bloch theory [2,3], the electronic structures of 3d-metal compounds have been a controversial topic of discussion. Many physicists have endeavoured to classify various 3d-metal compounds according to conductivity, and to understand the mechanism of that conductivity; especially, there has been interest in the reasons why NiO behaves as an insulator.

Mott [4] and Hubbard [5] suggested that the d–d Coulomb interaction energy U and d bandwidth w dominated the electronic structure near the Fermi level. If $U > w$, it is an insulator with the gap between the conduction band and valence band (as shown in figure 1) determined by the energy required for the fluctuations as $2d^n \rightarrow d^{n+1} + d^{n-1}$. In the case of $U < w$, it is a metal without a gap. From the experimental results that NiO is an insulator it has been believed to satisfy the former case, and is called a Mott insulator. The experimental results obtained by photoelectron spectroscopy (PES) and bremsstrahlung isochromat spectroscopy (BIS) were understood on the basis of the Mott–Hubbard model [6]; the main peak in PES was considered to be contributed by the d^7 state of Ni atoms, i.e. the lower Ni 3d band (valence band), and the satellite peaks corresponded to the O 2p band below the Ni 3d band. The above interpretation of the electronic structure has been considered to be effective for a long time.

Recently, Fujimori and Minami [7] and Sawatzky and Allen [8–10] pointed out the importance of the charge-transfer energy Δ from the O 2p band to the upper Ni 3d band (conduction band) and O 2p bandwidth W, as well as U and w, to the understanding of
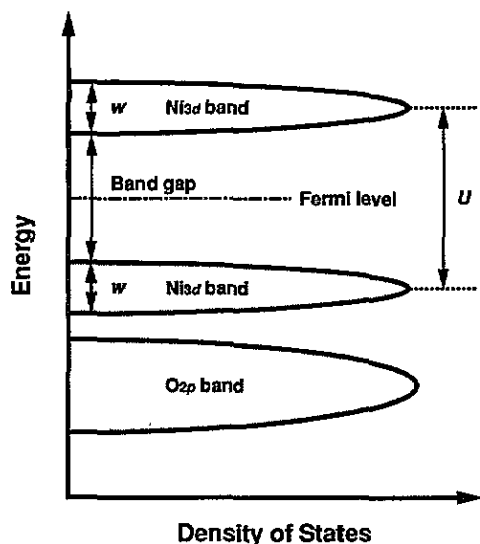
Figure 1. An artist's impression of NiO near the Fermi level based on a Mott-Hubbard type of electronic structure.
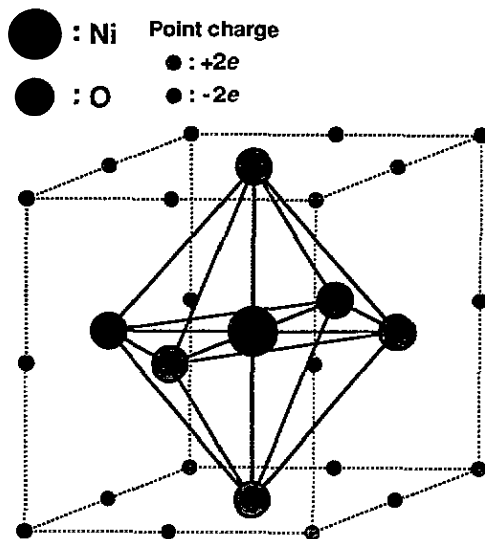
Figure 2. The structure of the unit cell situated in the centre of used finite unit cells. Small circles represent the point charges corresponding to Ni ions and O ions.

the electronic structure of NiO, especially the nature of the band gap. Sawatzky and Allen performed calculations with a semiempirical Anderson impurity Hamiltonian containing several fitting parameters such as orbital energies of d and p electrons, two centre parameters and Slater integrals. Fujimori and Minami used the configuration-interaction (CI) theory based on a similar Anderson impurity Hamiltonian and took Δ, U and transfer integrals as fitting parameters in order to obtain good agreement with the experimental results. They concluded that NiO was a charge-transfer-type insulator as Δ was smaller than U and that the O 2p band scarcely overlapped with the upper Ni 3d band, and they assigned the peaks in the PES spectra. The main peak of NiO observed in PES corresponds to the $d^8 L$ state, i.e. O 2p band, and the satellite peaks correspond mainly to the d^7 state, i.e. Ni 3d band. However, their methods have little ability to predict quantitatively the electronic structures without previous experiments.

From many previous works, the electronic structure of NiO was obtained using band calculations based on the local-density approximation (LDA) [11] of the density-functional theory [12, 13]. The results showed that NiO was a Mott–Hubbard type of insulator. The results were inconsistent with the experimental results [8, 10, 14] in the magnitude of the band gap between the valence band and conduction band. In general, LDA is thought to be inappropriate for the calculation of the electronic structure of late 3d transition-metal oxides. However, recently, according to the results obtained by Anisimov *et al* [15, 16] using band calculations (the so-called LDA+U method), the electronic structure of NiO was that of a charge-transfer-type insulator. The concept of this method was the same as that of the Anderson impurity model, namely to separate electrons into two subsystems. That is to say, d electrons were treated by a Hubbard-like term in the model Hamiltonian, and s and p electrons were described using LDA. Anisimov *et al* still used the model Hamiltonian.

A large amount of studies on the electronic structure of NiO were made using the molecular-orbital method appropriate for the localized orbital [17–22]. None were consistent with the obtained experimental results of the charge-transfer model. The drawbacks of the

previous methods are the use of small basis sets for atoms and the treatment of the Coulomb potential by consideration of the translational symmetry of the crystal by crystallography. In previous works, the adopted crystal potential (Madelung potential) made Ni 3d bands exist near the Fermi level. We think that the previous works cannot adequately reveal the electronic structure of NiO near the Fermi level without the assumption of a suitable crystal field.

Recently, it has become possible to perform a very large computation by an *ab initio* molecular-orbital method using a supercomputer in order to understand the electronic structure of materials. In the present paper, we report on the study of the electronic structure of a $[Ni-O_6]^{10-}$ cluster surrounded by several point charges in order to mimic the situation in a NiO crystal. We compare the calculated results with the previous works and the experimental results such as PES and BIS. Also, we discuss the physical property of NiO such as conductivity, and show that the order of the Ni 3d and O 2p bands play an important role in understanding the physical property of NiO, using the results of the cluster calculation. In addition, we investigate whether or not the use of point charges is appropriate to reflect the electronic structure of NiO.

2. Method

2.1. Calculated structure

In order to calculate the electronic structure of NiO composed of many atoms using an *ab initio* molecular-orbital method, we made the assumption that the electronic structure of a cluster made of finite unit cells could be representative of that of NiO mainly determined due to the localization effect of the Ni 3d atomic orbitals and the plane-wave-like character of the O 2p orbitals. Therefore, in the present analysis, we calculated the electronic structure of the following cluster model in place of NiO. Figure 2 shows the structure of the unit cell; the Ni–O bond length is 2.1 Å, according to the experimental result (2.09 Å) [17].

The calculated structure is composed of $3 \times 3 \times 3$ unit cells by consideration of the translational symmetry of the crystal by crystallography (the crystal structure of NiO is NaCl type). The $[Ni-O_6]^{10-}$ cluster was situated in the centre of the calculated structure, and the other Ni and O ions were replaced by point charges ($+2e$ for a Ni ion and $-2e$ for an O ion) surrounding the $[Ni-O_6]^{10-}$ cluster. Therefore, we could obtain information on the electronic structure of NiO by consideration of the interaction between Ni and O ions, but could not take account of the interaction between Ni ions.

2.2. Computational method

Using the GAUSSIAN 88 program package in the Cray Y-MP system [23], calculations were carried out by the unrestricted Hartree–Fock (UHF) method appropriate for the ground state of systems. The Hamiltonian based on non-relativistic quantum theory consists of the kinetic energy operator on electrons and Coulomb potential energy operator, which is composed of electron–nuclear attraction, electron–electron repulsion and nuclear–nuclear repulsion parts.

We used the basis sets for a Ni atom proposed by Roos *et al* [24], which gave results with high accuracy. Although each Ni 1s, 2s, 3s and 4s basis function is composed of a linear combination of 12 primitive Gaussian functions with appropriate contraction coefficients, the 10 largest contraction coefficients in the basis functions were chosen as contraction coefficients owing to the limitation of our program package. On the other hand, p and d basis functions were used as uncontracted. We used the basis set for O atoms (43/3) proposed by

Huzinaga *et al* as uncontracted [25]. We did not use the polarization and diffuse functions for both basis sets in order to reduce the computational time. In the present calculation, we used 192 primitive Gaussians (45 basis functions) for the $[Ni-O_6]^{10-}$ cluster.

Since the *ab initio* wavefunctions for this system consist of a single Slater determinant expanded by molecular orbitals made of the above basis functions, it can introduce the physical property generated by the localization effect of d electrons into the cluster model.

We calculated the electronic structure of the $[Ni-O_6]^{10-}$ cluster as follows. First, we treated the ground state of the $[Ni-O_6]^{10-}$ cluster as of high spin due to the fact that the exchange interaction stabilized the state of the system.

Next, the calculations of the two-electron integrals were carried out without regard to the symmetry of the point group O_h. Approximately 2000 self-consistent field (SCF) iterations were required, with the convergence criterion that the variation of the density matrix was within 10^{-7} to judge that the system was stabilized in energy. Finally, we obtained molecular orbitals, energies near the Fermi level and molecular coefficients mainly contributing to each molecular orbital. We performed Mulliken population analysis using the SCF density in order to find the gross orbital populations, the charge distribution of the system and the spin distribution on each ion, and to understand the state of the bonding between Ni and O ions.

3. Computational results and discussion

3.1. Computational results

Owing to the fact that experimental data show that the spin magnetic moment for the Ni ion in NiO is not $2.0\mu_B$ but $1.77\mu_B$ [26], $1.64\mu_B$ [27] or $1.90\mu_B$ [28], we calculated the electronic states of the $[Ni-O_6]^{10-}$ cluster corresponding to both the $t_{2g\uparrow}^3 t_{2g\downarrow}^3 e_{g\uparrow}^2 e_{g\downarrow}^1$ and $t_{2g\uparrow}^3 t_{2g\downarrow}^3 e_{g\uparrow}^2$ configurations. The obtained results are described as follows.

First, we show the calculated results of the electronic states corresponding to the $t_{2g\uparrow}^3 t_{2g\downarrow}^3 e_{g\uparrow}^2 e_{g\downarrow}^1$ configuration. The obtained results are listed in table 1 for up spin and in table 2 for down spin due to the UHF method, which gives the different orbitals for different spins (the molecular orbitals with relatively small coefficients were neglected). The obtained discrete molecular energy levels are considered to form the continuous energy bands.

Molecular orbitals 1, 2, 3–5, 6–11, 12, 13–15 and 16–22 for both up and down spins correspond to Ni 1s, Ni 2s, Ni 2p, O 1s, Ni 3s, Ni 3p and O 2s orbitals, respectively, i.e. those related to core electrons.

In table 1, molecular orbitals 23–44 (occupied orbitals) and molecular orbital 45 (unoccupied orbital) are listed. According to the band picture, we can consider those orbitals as follows. The molecular orbitals 23–28 and 33–34 form the lower Ni 3d band, which consists of the split 3d orbitals never caused by the spin–orbit interaction [29], which was not automatically included in the present analysis based on the non-relativistic quantum theory (the molecular orbitals 33–34 have a small contribution to the lower Ni 3d band). The molecular orbitals 28–34 form the lower O 2p band, and the molecular orbitals 35–44 form the upper O 2p band. Molecular orbital 45 forms the Ni 4s band.

Similarly, in table 2, molecular orbitals 23–42 (occupied orbitals) and molecular orbitals 43–45 (unoccupied orbitals) are listed. According to the band picture, the molecular orbitals 23–27 and 32 are the lower Ni 3d band, which consists of the split 3d orbitals (the molecular orbital 32 has a small contribution to the lower Ni 3d band). The molecular orbitals 26–32

Table 1. Molecular orbitals and their energies for up spin in $t_{2g\uparrow}^3 t_{2g\downarrow}^3 e_{g\uparrow}^2 e_{g\downarrow}^1$ configuration (energy is in Hartree).

Molecular-orbital number	Energy	Ni s	Ni d	O p
23	−1.498 29		$3d_{3z^2-r^2}$, $3d_{x^2-y^2}$	
24	−1.490 24		$3d_{xz}$	
25	−1.466 73		$3d_{yz}$	
26	−1.465 97		$3d_{xy}$	
27	−1.420 68		$3d_{3z^2-r^2}$, $3d_{x^2-y^2}$	
28	−1.363 60		$3d_{yz}$	$2p_z$
29	−1.308 82			$2p_x$, $2p_z$
30	−1.290 62			$2p_x$
31	−1.238 94			$2p_z$
32	−1.223 08			$2p_x$
33	−1.187 60		$3d_{3z^2-r^2}$	$2p_x$, $2p_z$
34	−1.149 68		$3d_{x^2-y^2}$	$2p_x$, $2p_y$
35	−0.854 41			$2p_x$, $2p_z$
36	−0.850 59			$2p_y$
37	−0.848 37			$2p_y$
38	−0.844 84			$2p_x$
39	−0.832 65			$2p_y$
40	−0.831 77			$2p_y$
41	−0.831 27			$2p_z$
42	−0.816 07			$2p_x$, $2p_z$
43	−0.774 91			$2p_z$
44	−0.773 56			$2p_x$
45	−0.506 07	4s		

form the lower O 2p band, and the molecular orbitals 33–42 form the upper O 2p band. The molecular orbitals 43–45 form the conduction band, and especially molecular orbital 45 forms the upper Ni 3d band.

As we used a cluster model to understand the electronic structure of NiO, the obtained results include unphysical states on Ni 4s and O 2p bands. They were understood in the following.

The molecular orbital 44 consisting of Ni 4s atomic orbitals for down spin is lower than that of NiO, because of the attractive interaction between Ni 4s electrons and the positive point charges ($+2e$) representing the Ni ions, which causes the energy of this molecular orbital to be much lower than the energy of the Ni 4s electrons in bulk NiO without regard for the electron repulsion between 4s and 3d electrons. Also the energy of molecular orbital 43 consisting of O 2p atomic orbitals for down spin is lower than that of NiO. In fact, molecular orbital 43 mixes with molecular orbital 45 in the same energy region.

Therefore, the upper Ni 3d band consists of some parts of $3d_{3z^2-r^2}$ and $3d_{x^2-y^2}$ (e_g orbitals), and the lower Ni 3d band consists of some of the remaining parts of $3d_{3z^2-r^2}$ and $3d_{x^2-y^2}$ and all of $3d_{xy}$, $3d_{xz}$ and $3d_{yz}$ (t_{2g} orbitals). The energies of e_g orbitals are higher than those of t_{2g} orbitals by consideration of the electrostatic interaction between each orbital and O ions.

The energy difference between molecular orbitals 42 and 45 is large (8.2 eV). The $t_{2g\uparrow}$ and $e_{g\uparrow}$ orbitals are lower than those for down spins. The exchange splitting is about 1 eV.

According to the Mulliken population analysis of the cluster, the electron occupation number of Ni 3d is 9.0, being 5.0 for the up spin state and 4.0 for the down spin state. The average net charges of Ni and O are $+0.53e$ and $-1.73e$ (in this case, the net charge of two O ions is $-1.5e$, other O ions $-2.0e$), respectively, according to the obtained results

Table 2. Molecular orbitals and their energies for down spin in $t_{2g\uparrow}^3 t_{2g\downarrow}^3 e_{g\uparrow}^2 e_{g\downarrow}^1$ configuration (energy is in Hartree).

Molecular-orbital number	Energy	Ni s	Ni d	O p
23	−1.469 07		$3d_{xz}$	
24	−1.428 61		$3d_{xy}$	
25	−1.419 83		$3d_{yz}$	
26	−1.386 59		$3d_{3z^2-r^2}$, $3d_{x^2-y^2}$	$2p_x$
27	−1.298 89		$3d_{3z^2-r^2}$, $3d_{x^2-y^2}$	$2p_y$, $2p_z$
28	−1.253 03		.	$2p_x$
29	−1.231 72			$2p_x$, $2p_z$
30	−1.229 61			$2p_z$
31	−1.212 90			$2p_x$
32	−1.144 85		$3d_{3z^2-r^2}$, $3d_{x^2-y^2}$	$2p_y$
33	−0.852 30			$2p_x$, $2p_z$
34	−0.842 51			$2p_x$
35	−0.833 82			$2p_y$
36	−0.832 85			$2p_y$
37	−0.830 79			$2p_y$
38	−0.830 04			$2p_z$
39	−0.826 84			$2p_y$
40	−0.814 48			$2p_x$, $2p_z$
41	−0.773 25			$2p_x$
42	−0.770 17			$2p_z$
43	−0.590 85			$2p_z$
44	−0.495 84	4s		
45	−0.469 42		$3d_{3z^2-r^2}$, $3d_{x^2-y^2}$	

that the energies of Ni 4s levels in the finite cluster are much lower and that the energies of O 2p energy levels are much higher compared with those in NiO. The electronic state of the $[\text{Ni–O}_6]^{10-}$ cluster in the $t_{2g\uparrow}^3 t_{2g\downarrow}^3 e_{g\uparrow}^2 e_{g\downarrow}^1$ configuration corresponds to $d^9 L$, caused by the lower Ni 3d band heavily mixed with the lower O 2p band.

Secondly, we show the calculated results of the electronic states corresponding to the $t_{2g\uparrow}^3 t_{2g\downarrow}^3 e_{g\uparrow}^2$ configuration as shown in table 3 for up spin and in table 4 for down spin. In table 3, molecular orbitals 22–44 (occupied orbitals) and molecular orbital 45 (unoccupied orbital) are listed. The molecular orbitals 22–26 and 31–32 are viewed as the lower Ni 3d band (the molecular orbitals 31–32 have a small contribution to the lower Ni 3d band). The molecular orbitals 27–32 form the lower O 2p band, and the molecular orbitals 33–44 form the upper O 2p band. The molecular orbital 45 forms the Ni 4s band.

In table 4, the molecular orbitals 22–42 (occupied orbitals) and molecular orbitals 43–45 (unoccupied orbitals) are listed. Molecular orbitals 22–24 and 26–27 are considered as the lower Ni 3d band, which consists of the split 3d orbitals. Molecular orbitals 25–30 form the lower O 2p band, and molecular orbitals 31–42 form the upper O 2p band. The molecular orbitals 43–44 form the upper Ni 3d band. The molecular orbital 45 is regarded as the Ni 4s band.

The energy difference between the top of the upper O 2p band and the bottom of the upper Ni 3d band is small (0.7 eV). The electron occupation number of Ni 3d is 8.7, i.e. 5.0 for the up spin state and 3.7 for the down spin state. The average net charges of Ni and O are $+0.84e$ and $-1.81e$ (in this case, the net charge of each O ion is the same), respectively. The electronic state of the $[\text{Ni–O}_6]^{10-}$ cluster in the $t_{2g\uparrow}^3 t_{2g\downarrow}^3 e_{g\uparrow}^2$ configuration corresponds to d^8.

From the calculation of the electronic structure of the $[\text{Ni–O}_6]^{10-}$ cluster in both

Table 3. Molecular orbitals and their energies for up spin in $t_{2g\uparrow}^3 t_{2g\downarrow}^3 e_{g\uparrow}^2$ configuration (energy is in Hartree).

Molecular-orbital number	Energy	Ni s	Ni d	O p
22	−1.74107		$3d_{xy}$, $3d_{xz}$, $3d_{yz}$	
23	−1.74107		$3d_{xy}$, $3d_{xz}$, $3d_{yz}$	
24	−1.74107		$3d_{xy}$, $3d_{xz}$, $3d_{yz}$	
25	−1.68312		$3d_{3z^2-r^2}$	
26	−1.68312		$3d_{x^2-y^2}$	
27	−1.41299			$2p_x$, $2p_y$, $2p_z$
28	−1.30727			$2p_y$
29	−1.30727			$2p_z$
30	−1.30727			$2p_x$
31	−1.27492		$3d_{3z^2-r^2}$	$2p_z$
32	−1.27492		$3d_{x^2-y^2}$	$2p_y$
33	−0.91842			$2p_x$, $2p_z$
34	−0.91842			$2p_y$, $2p_z$
35	−0.91842			$2p_x$, $2p_y$
36	−0.90412			$2p_x$
37	−0.90412			$2p_z$
38	−0.90412			$2p_x$
39	−0.89981			$2p_x$, $2p_y$
40	−0.89981			$2p_y$
41	−0.89981			$2p_z$
42	−0.88145			$2p_y$, $2p_z$
43	−0.88145			$2p_x$, $2p_z$
44	−0.88145			$2p_x$, $2p_y$
45	−0.55625	4s		

configurations, we also obtained the result that the molecular orbitals assigned to O 2p existed between those assigned to Ni 3d. The electronic structures in both configurations are similar except for the energy difference between the top of the upper O 2p band and the bottom of upper Ni 3d band.

We obtained the results that the energy of Ni ions in $t_{2g\uparrow}^3 t_{2g\downarrow}^3 e_{g\uparrow}^2$ configuration is slightly higher than that in $t_{2g\uparrow}^3 t_{2g\downarrow}^3 e_{g\uparrow}^2 e_{g\downarrow}^1$ configuration.

3.2. The electronic structure of NiO

3.2.1. Local density of states of NiO. From tables 1 and 2, the electronic structure of NiO near the Fermi level derived from the calculation of that of a $[\text{Ni–O}_6]^{10-}$ cluster surrounded by several point charges is summarized by using LDOS as an artist's impression of the obtained electronic state for up and down spins in figure 3(a) and the total electronic state in figure 3(b). The upper Ni 3d band in up spin state is not shown, because it was not derived from the present calculation using the $[\text{Ni–O}_6]^{10-}$ cluster with Ni up spin.

LDOS concerning Ni 3d and O 2p bands exist mainly in the range of 30 eV near the Fermi level. The bandwidth of the upper O 2p band is narrower than that of the lower O 2p band, but the upper O 2p band has higher LDOS than the lower O 2p band. The bandwidth of the lower Ni 3d band is broader than that of the upper O 2p band.

The obtained results as shown in figure 3(b) are consistent with the experimental results obtained by Sawatzky as shown in figure 4 [10], except for the absolute value of the position of the main peak and satellite of the spectral distribution and the magnitude of the band gap. (We did not consider the cross section of photoemission to represent the shape of spectra and did not use Green function methods.)

Table 4. Molecular orbitals and their energies for down spin in $t_{2g\uparrow}^3 t_{2g\downarrow}^3 e_{g\uparrow}^2$ configuration (energy is in Hartree).

| Molecular-orbital number	Energy	Ni s	Ni d	O p
22	−1.695 46		$3d_{xy}, 3d_{xz}, 3d_{yz}$	
23	−1.695 46		$3d_{xy}, 3d_{xz}, 3d_{yz}$	
24	−1.695 46		$3d_{xy}, 3d_{xz}, 3d_{yz}$	
25	−1.366 02			$2p_x, 2p_y, 2p_z$
26	−1.310 01		$3d_{3z^2-r^2}$	$2p_z$
27	−1.310 01		$3d_{x^2-y^2}$	$2p_x, 2p_y$
28	−1.223 79			$2p_x$
29	−1.223 79			$2p_y$
30	−1.223 79			$2p_z$
31	−0.912 66			$2p_y, 2p_z$
32	−0.912 66			$2p_x, 2p_z$
33	−0.912 66			$2p_x, 2p_y$
34	−0.898 16			$2p_x$
35	−0.898 16			$2p_y$
36	−0.898 16			$2p_z$
37	−0.894 24			$2p_y$
38	−0.894 24			$2p_x$
39	−0.894 24			$2p_z$
40	−0.875 80			$2p_y, 2p_z$
41	−0.875 80			$2p_x, 2p_z$
42	−0.875 80			$2p_x, 2p_y$
43	−0.850 18		$3d_{3z^2-r^2}$	$2p_z$
44	−0.850 18		$3d_{x^2-y^2}$	$2p_x, 2p_y$
45	−0.523 80	4s		
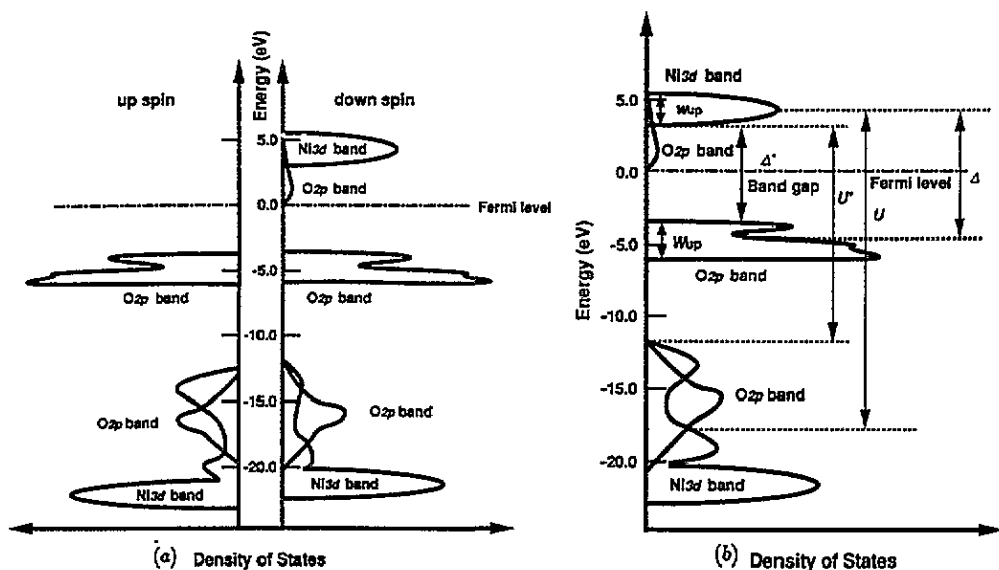
Figure 3. An artist's impression of the obtained electronic structure of NiO near the Fermi level derived from the cluster model calculations ($t_{2g\uparrow}^3 t_{2g\downarrow}^3 e_{g\uparrow}^2 e_{g\downarrow}^1$ configuration): (*a*) for up and down spins and (*b*) for total spins.
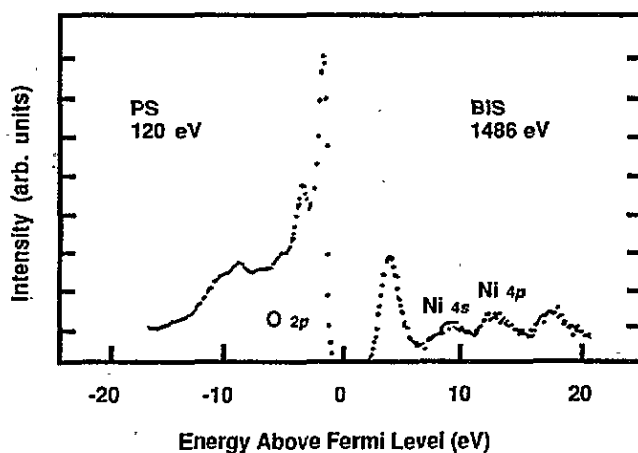
Figure 4. Experimental results obtained by photoelectron spectroscopy (PS) and bremsstrahlung isochromat spectroscopy (BIS) [10].

According to the above results, we concluded that the main features of NiO were similar to those of the cluster. Nieuwpoort and Broer [30] indicated that calculations of the cluster model embedded in the remaining part of the Madelung potential and short-range Born repulsion potential were similar to the band calculations of the crystal from the localized Wannier picture. We obtained results that supported their indication, while our calculations did not include the effect of the short-range Born repulsion potential.

3.2.2. The band gap. We can discuss the problem of the band gap by using the results in the $t_{2g\uparrow}^3 t_{2g\downarrow}^3 e_{g\uparrow}^2 e_{g\downarrow}^1$ configuration.

The magnitude of the gap E_g between conduction band and valence band plays an important role in the determination of the electronic conductivity of NiO. In general, the calculation of the magnitude of the band gap necessitates consideration of terms including the many-body effects; these are the interaction between core holes and the other electrons containing the screening effects due to electronic correlation, the finite lifetime of the core holes and the scattering process of electrons. However, we neglected the above consideration for simplicity. We tried to make a qualitative understand of the band gap using the following simple model.

E_g is derived from the formula that

$$E_g = E_{n+1} + E_{n-1} - 2E_n \tag{1}$$

where E_n, E_{n+1} and E_{n-1} are the total energy corresponding to the ground state of the system containing n, $n + 1$ and $n - 1$ electrons derived from calculating the ground state of the $[Ni-O_6]^{10-}$, $[Ni-O_6]^{11-}$ (electron addition) and $[Ni-O_6]^{9-}$ (electron removal) clusters, respectively. (The ground state of the $[Ni-O_6]^{9-}$ cluster is mainly d^9L^2, and the present $[Ni-O_6]^{9-}$ cluster calculation led to the excess O 2p hole in the ground state of the system. The ground state of the $[Ni-O_6]^{11-}$ cluster is d^9.)

We obtained that E_g is 9.9 eV (0.36 Hartree), which is much larger than the experimental results obtained by PES and BIS (for example, 4.3 eV reported by Zaanen *et al* [9]). This is due to the fact that electron correlation was not taken into account in the present analysis, and that the point charges representing the atoms around the $[Ni-O_6]^{10-}$ cluster were not sufficient to give the ionization energy and the electron affinity.

We compared the experimental band gap with the calculated value from tables 1 and 2. We defined that the Fermi level exists in the middle of molecular orbitals 42 and 45. The p–d transition energy Δ' was derived from the energy difference between the molecular orbital 42 corresponding to the top of the upper O 2p band and the molecular orbital 45 corresponding to the bottom of the upper Ni 3d band in table 2 (the bandwidth of the upper Ni 3d band is neglected, as it is less than 1 eV). According to Koopmans theorem, the obtained Δ' value is 8.2 eV (0.03 Hartree). In similar manner, we obtained the p–d transition energy Δ, the d–d transition energy U' and the d–d transition energy U as listed in table 5. While the band above the Fermi level (the upper Hubbard band) consists of the Ni 3d and O 2p orbitals, the O 2p orbitals have smaller contribution to this upper Hubbard band than the Ni 3d orbitals.

Table 5. Comparison between computational and experimental transition energies (energy is in eV).

	p–d transition energy		d–d transition energy	
	Δ	Δ'	U	U'
Calc.	9.3	8.2	22.8	18.4
Expt.	—	4.0	—	13.0

Hence, both Δ and Δ' are smaller than U and U'. Δ' and U' are also a little larger than the observed values (on the contrary, Janssen *et al* obtained results that Δ is almost equal to U). The calculated values are larger than the experimental values. In Koopmans theorem, the effect of the redistribution of electrons was not taken into account. We think that methods containing electron correlation, such as CI method, Moller–Plesset correlation energy calculation and so on, will be able to give computational results with higher accuracy.

3.2.3. Interpretation of PES and BIS data. We interpreted the PES and BIS data shown in figure 4 as follows. The main peak of NiO observed in PES corresponds to the $d^8 L$ state, i.e. O 2p bands, and the satellite peaks correspond mainly to the mixed state produced by the correlation between the 2p state of O atoms and the d^8 state of Ni atoms. Our explanation differs from that of the conventional Mott–Hubbard theory in the order of Ni 3d and O 2p bands. In addition, local excitation with the interaction between electrons and holes (from results that holes exist in O ions) partially contributes to these satellite peaks.

NiO can be classified by the terms such as Δ, U and so on as follows. NiO is not a conventional Mott–Hubbard type of insulator ($\Delta > U$), but a charge-transfer-type insulator ($\frac{1}{2}(w_{up} + W_{up}) < \Delta < U$) in terms of the Zaanen–Sawatzky–Allen phase diagram [9], where w_{up} and W_{up} are the bandwidths of the upper Ni 3d and the upper O 2p bands, respectively. Then, we found that the magnitude of the band gap of NiO was not determined by U but Δ, and that the band gap emerged due to a p–d transition between Ni and O ions. The interaction between Ni 3d and O 2p plays an important role in determining the electronic structure of NiO.

3.2.4. The interpretation of the obtained electronic structure. The obtained electronic structure of NiO derived from the cluster calculations differs much from those of previous works in the calculations of band structures. For instance, Brener *et al* obtained the results that the upper Ni 3d band was above the Fermi level and the lower Ni 3d and the O 2p bands were below the Fermi level, and that the mixing of the Ni 3d and O 2p bands were

very small [19]. Sawatzky *et al* never predicted that the O 2p band consists of two split bands. The splitting of 3d orbitals in Ni 3d band is also observed in the previous results without including the spin–orbit interaction. The splitting seems to arise due to the crystal field and the effect of band mixing.

However, recently, the self-interaction correction (SIC) to LDA applied by Svane and Gunnarsson gave a great improvement in the calculation of the band gap [31]. They obtained the magnitude of band gap of NiO as 2.54 eV. The UHF method is intrinsically self-interaction-free. Their results are consistent with our results.

Our results are also in qualitative agreement with that of Anisimov *et al* [15, 16] in that NiO satisfies the relation $\frac{1}{2}(w_{up} + W_{up}) < \Delta < U$, because the adopted UHF approximation involved the exact exchange energy and their method contained the exchange energy with good accuracy. We obtained the result that there was the mixing of the Ni 3d and O 2p bands below the Fermi level similar to that of Anizimov *et al*. However, their results show larger hybridization of the Ni 3d and O 2p bands than ours. Some of the lower Ni 3d bands are pulled up to the top of the valence band and mix with the O 2p bands. We also obtained the similar splitting of the O 2p bands. In a similar way, the upper Ni 3d and O 2p orbitals contribute to the bands above the Fermi level.

According to the cluster calculations, we obtained the results that the average charge of O ions was $-1.73e$, and the ground state of NiO was d^9L. These results differ from the previous results, which concluded that the average charge of O ion was about $-1.9e$, NiO was a fully ionic compound, and the ground state was d^8 predicted by the Mott–Hubbard theory [17–22]. Even if we took into account the incompleteness of the basis sets and Hartree–Fock method, Illas *et al* showed that NiO was an ionic compound with a small contribution to the covalent bonding between a Ni ion and an O ion [32]. According to the Mulliken population analysis for the density matrix, the obtained overlapping of Ni e_g orbitals and O 2p orbitals is so large that it causes a superexchange interaction between Ni ions via O ions [33]. The t_{2g} orbitals scarcely mix with the O 2p orbitals. We think that charge transfer between Ni and O ions will occur via such hybridization.

From the above discussion, we can explain the reason why the O 2p bands are above the lower Ni 3d band. The bondings between Ni 3d and the nearest O 2p orbitals are ionic with some covalency. The interaction between Ni 3d and the remaining Ni 3d or O 2p orbitals are fully ionic. Unlike the traditional idea, the nearest O 2p ions are not solely the origin of negative charge for a given Ni ion. Therefore, the energy level of the lower Ni 3d band cannot be pulled up to near the Fermi level and the O 2p bands exist above the lower Ni 3d band.

Now, we think that the present calculation using the point charges around the $[Ni–O_6]^{10-}$ cluster causes this state to have one O 2p hole at most (the electron occupation number of Ni 4s is neglected), because the cluster model in the present analysis like the $[Ni–O_6]^{10-}$ cluster was inadequate to describe charge transfer between Ni and O ions. A cluster model of large size may be necessary. Consequently, appropriate charge distribution for Ni and O ions occurs to stabilize the system, and we will never obtain the result of the existence of the excess O 2p hole.

The physical picture of NiO derived from the calculation of electronic structure is the following. In the case when the band gap becomes zero by hole doping ($\frac{1}{2}(w_{up} + W_{up}) > \Delta$, $\Delta < U$), electrons move indirectly between Ni ions via an O ion rather than directly between Ni ions, i.e. the fluctuation of O as well as Ni ions causes electrons to move with a complicated interaction between the generated holes and electrons. In fact, the above explanation easily also leads to understanding of the phenomenon of Li-doped NiO that Li doping pulls the Fermi level into O ligand band and eventually it behaves as a p metal.

From the physical picture of the magnetic property of NiO, the obtained large U naturally leads to the antiferromagnetic nature of NiO. By hole doping, NiO loses the characteristics of antiferromagnetism. Therefore, our obtained results provide the consistency between the conductivity and magnetism of NiO. The obtained spin magnetic moment is $1.0\mu_B$ because of the ground state of NiO being d^9L. This value is similar to that of Terakura *et al* (their obtained spin magnetic moment was $1.04\mu_B$) [12], which it seems to be smaller than those in the real crystal.

3.3. Evaluation of Coulomb potential generated by point charges

In order to investigate whether or not the geometrical arrangement of point charges adopted in the present analysis was appropriate for reflecting the electronic structure of NiO, we calculated the electronic structures of the $[Ni-O_6]^{10-}$ cluster with some types of geometrical arrangement of point charges (with $2 \times 2 \times 2$ unit cells and with $7 \times 7 \times 7$ unit cells). Similar results were obtained to those in the case of $3 \times 3 \times 3$ unit cells. That is to say, the lower Ni 3d band energy is lower than those of the O 2p bands. Therefore, if there are a sufficient number of point charges corresponding to both Ni^{2+} and O^{2-} around the adopted cluster, the electronic structure of the $[Ni-O_6]^{10-}$ cluster changes slightly.

Now, we tried to examine the validity of the employed fractional point charges in previous work done by Shashkin and Goddard [34] and Brener and Callaway [19]. Brener *et al* adopted the method to make the cluster electrically neutral by adding 12 point charges with $+\frac{5}{6}e$ at the positions of the 12 second-nearest neighbours of Ni–O in order to obtain convergence of the SCF calculation. Using the above fractional point charges, we obtained the results that the upper Ni 3d band was above the Fermi level, and that the lower Ni 3d and O 2p bands were below the Fermi level. This result showed that NiO is a Mott-Hubbard type of insulator. However, the existence of O ions was not taken into account in this method, while the Coulomb force among point charges has an effect even at long range. This method seems to be inappropriate for the evaluation of the Coulomb potential. On the other hand, we think that our method containing this effect is suitable for the calculation of electronic structures. That is to say, adopting alternating positive and negative charges led to good results.

We examined the variation of the electronic structures in the case of charge neutrality of the used cluster by choosing the appropriate boundary condition that fractional ($\frac{1}{2}$, $\frac{1}{4}$ and $\frac{1}{8}$) charges were positioned on faces, edges and corners, respectively, in the outer of the whole cells in order to satisfy charge neutrality. We found that the variation of the electronic structures was very small.

Hence, it is sufficient to discuss the electronic structures of NiO derived from the assumption that NiO is a fully ionic compound. However, we notice that NiO is an ionic compound with covalent bonding, according to the small mixing of the Ni 3d and O 2p orbitals found in tables 1 and 2. Therefore, we also tried to investigate how the magnitude of the arranged point charges influenced the electronic structures of the $[Ni-O_6]^{10-}$ cluster, by cluster calculations using the magnitude of charges with $1.6e$, $1.4e$ for Ni, and $-1.6e$, $-1.4e$ for O, respectively. The obtained electronic structures were almost the same as those in the case of $2.0e$ for Ni and $-2.0e$ for O. From the above results, the use of point charges in the present analysis is suitable for reflecting the electronic structure of NiO by using cluster calculations.

4. Conclusion

We calculated the electronic structure of the $[Ni-O_6]^{10-}$ cluster surrounded by several point

charges in order to mimic the situation in a NiO crystal using the *ab initio* molecular-orbital method. We showed that the obtained density of states agreed reasonably well with experimental results. The above results led to the conclusion that main electronic structures of NiO were similar to those of the cluster, due to the interaction of Ni atoms with surrounding O atoms rather than the Ni–Ni interaction.

We obtained the results that NiO was an insulator with a band structure where the upper Ni 3d band, which contained a small contribution of the O 2p orbital, was above the Fermi level, and the upper O 2p, the lower O 2p and the lower Ni 3d bands were below the Fermi level, and had the electronic structures derived from the charge-transfer model proposed by Sawatzky and Allen. The main peak observed in PES corresponds to the $d^8 L$ states, i.e. O 2p band, and the satellite peaks correspond mainly to the mixed state produced by the correlation between the 2p state of O atoms and the d^8 state of Ni atoms.

The present analysis of the electronic state of the cluster, using *ab initio* calculations based on the independent electron theory without regard for the Coulomb correlation, enables us to understand the main features of valence electronic structures of NiO due to the following points: (i) adopting the large basis sets for Ni atoms, (ii) using the appropriate point charges representing the crystal Coulomb potential by consideration of the translational symmetry of crystal, and (iii) taking into account the interaction of Ni atoms with the surrounding O atoms, which is an important factor in determining the electronic structures of NiO. We think that our method can be extensively available to understand the qualitative physical property of other metal oxides such as CuO, CoO and FeO.

Finally, our method is still insufficient to give the quantitative description of valence band structures of 3d metal oxides such as NiO because of neglect of the 3d–3d interaction and of using the insufficient approximation for correlation effect such as the 3d Coulomb repulsion. It is necessary to build up the new method.

Acknowledgments

References

[1]   de Boer S H and Verwey E J W 1937 *Proc. Phys. Soc.* A **49** 59
[2]   Wilson A H 1931 *Proc. R. Soc.* A **133** 458
[3]   Bloch F 1929 *Z. Phys.* **57** 545
[4]   Mott N F 1949 *Proc. R. Soc.* A **62** 416
[5]   Hubbard J 1963 *Proc. R. Soc.* A **276** 238
[6]   McKay J M and Henrich V E 1984 *Phys. Rev. Lett.* **53** 2343
[7]   Fujimori A and Minami F 1984 *Phys. Rev.* B **30** 957
[8]   Sawatzky G A and Allen J W 1984 *Phys. Rev. Lett.* **53** 2239
[9]   Zaanen J, Sawatzky G A and Allen J W 1986 *J. Magn. Magn. Mater.* **54–57** 607
[10] Sawatzky G A 1988 *Springer Series in Solid-State Science* vol 81 (Berlin: Springer)
[11] Kryachko E S and Ludena E V 1990 *Energy Density Functional Theory of Many-Electron Systems* (Dordrecht: Kluwer Academic)
[12] Terakura K, Oguchi T, Williams A R and Kuebler J 1984 *Phys. Rev.* B **30** 4734
[13] Shen Z-X, List R S, Dessau D S, Wells B O, Jepsen O, Arko A J, Barttlet R, Shih C K, Parmigiani F, Huang J C and Lindberg P A P 1991 *Phys. Rev.* B **44** 3604
[14] Hüfner S and Riesterer T 1986 *Phys. Rev.* B **33** 7267
[15] Anisimov V I, Zaanen J and Andersen O K 1991 *Phys. Rev.* B **44** 943

[16] Anisimov V I, Solovyev I V, Korotin M A, Czyzyk M T and Sawatzky G A 1993 *Phys. Rev.* B **48** 169 29
[17] Surratt G T and Kunz A B 1977 *Solid State Commun.* **23** 555
[18] Bagus P S and Wahlgren U 1977 *Mol. Phys.* **33** 641
[19] Brener N E and Callaway J 1987 *Phys. Rev.* B **35** 4001
[20] Janssen G J M and Nieuwpoort W C 1988 *Phys. Rev.* B **38** 3449
[21] Janssen G J and Nieuwpoort W C 1988 *Int. J. Quantum Chem.* **22** 679
[22] Pacchioni G, Bagus P S and Parmigiani F 1992 *Cluster Models for Surface and Bulk Phenomena* (New York: Plenum)
[23] Frisch M J *et al* 1988 *Gaussian 88* (Pittsburgh, PA: Gaussian Inc.)
[24] Roos B, Veillard A and Vinot G 1971 *Theor. Chim. Acta.* **20** 1
[25] Huzinaga S, Andzelm J, Klobukowski M, Radzio-Andzelm E, Sakai Y and Tatewaki H 1984 *Physical Sciences Data: 16 Gaussian Basis Sets for Molecular Calculations* (Amsterdam: Elsevier)
[26] Fender B E F, Jacobson A J and Wegwood F A 1968 *J. Chem. Phys.* **48** 990
[27] Alperin H A 1962 *J. Phys. Soc. Japan Suppl.* B **17** 12
[28] Cheethan A K and Hope D A O 1983 *Phys. Rev.* B **27** 6964
[29] Schaeffer III H F 1977 *Applications of Electronic Structure Theory* (New York: Plenum)
[30] Nieuwpoort W C and Broer R 1992 *Cluster Models for Surface and Bulk Phenomena* (New York: Plenum) p 505
[31] Svane A and Gunnarsson O 1990 *Phys. Rev. Lett.* **65** 1148
[32] Illas F, Lorda A, Rubio J, Torrance J B and Bagus P S 1993 *J. Chem. Phys.* **99** 389
[33] Anderson P W 1959 *Phys. Rev.* **115** 2
[34] Shashkin S Y and Goddard III W A 1986 *Phys. Rev.* B **33** 1353